molecular pharmaceutics

Article

Cite This: Mol. Pharmaceutics 2019, 16, 3842−3852

pubs.acs.org/molecularpharmaceutics

P-glycoprotein Limits Ribociclib Brain Exposure and CYP3A4 Restricts Its Oral Bioavailability

Alejandra Martínez-Chávez,[†,‡] Stéphanie van Hoppe,[†] Hilde Rosing,[‡] Maria C. Lebre,[†] Matthijs Tibben,[‡] Jos H. Beijnen,[†,‡,§] and Alfred H. Schinkel*[,†]

[†]Division of Pharmacology, The Netherlands Cancer Institute, Amsterdam, The Netherlands

[‡]Department of Pharmacy & Pharmacology, The Netherlands Cancer Institute, Amsterdam, The Netherlands

[§]Division of Pharmacoepidemiology and Clinical Pharmacology, Utrecht Institute for Pharmaceutical Sciences, Utrecht University, Utrecht, The Netherlands

Supporting Information

ABSTRACT: Ribociclib is a CDK4/6 inhibitor recently approved for the treatment of some types of breast cancer in combination with an aromatase inhibitor. It is currently investigated in the clinic to treat other malignancies, including brain tumors. Using *in vitro* and genetically modified mouse models, we investigated the effect of the multidrug efflux transporters ABCB1 and ABCG2, and the drug-metabolizing CYP3A enzymes on ribociclib pharmacokinetics and tissue distribution. *In vitro*, ribociclib was avidly transported by human ABCB1, but not by human ABCG2 and only modestly by mouse Abcg2. Upon oral administration at 20 mg/kg, the plasma AUC_{0-24h} of ribociclib was increased by 2.3-fold, and its terminal elimination was delayed in *Abcb1a/1b*$^{-/-}$;*Abcg2*$^{-/-}$ compared to wild-type mice. The brain-to-plasma ratios of ribociclib were increased by at least 23-fold relative to wild-type mice in *Abcb1a/1b*$^{-/-}$;*Abcg2*$^{-/-}$ and *Abc1a/1b*$^{-/-}$ mice, but not noticeably in *Abcg2*$^{-/-}$ mice. Oral coadministration of elacridar, an ABCB1 and ABCG2 inhibitor, increased the brain penetration of ribociclib in wild-type mice to the same level as seen in *Abcb1a/1b*$^{-/-}$;*Abcg2*$^{-/-}$ mice. Plasma exposure of ribociclib further decreased by 3.8-fold when transgenic human CYP3A4 was overexpressed in *Cyp3a*-deficient mice. Ribociclib penetration into the brain is thus drastically limited by ABCB1 in the blood−brain barrier, but coadministration of elacridar can fully reverse this process. Moreover, human CYP3A4 can extensively metabolize ribociclib and strongly restrict its oral bioavailability. The insights obtained from this study may be useful to further optimize the clinical application of ribociclib, especially for the treatment of (metastatic) brain tumors.

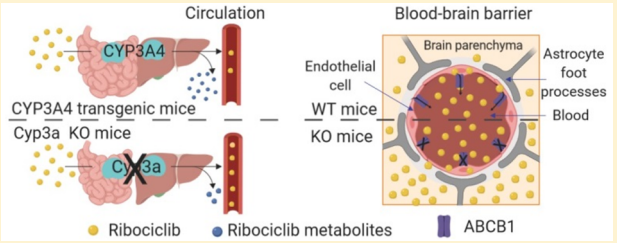

KEYWORDS: *ribociclib, CDK4/6 inhibitor, P-gp, BCRP, CYP3A4, brain penetration*

INTRODUCTION

In recent years, a new class of compounds was successfully introduced in the clinic for breast cancer treatment. These are inhibitors of the cyclin-dependent kinases 4 and 6 (CDK4/6), enzymes that regulate cell cycle progression through the G1/S transition.[1] To date, three CDK4/6 inhibitors have been approved by the US Food and Drug Administration (FDA) and the European Medicines Agency (EMA): palbociclib (2015), ribociclib (2017), and abemaciclib (2017−2018). These compounds are registered for the treatment of advanced-stage and/or metastatic hormone receptor-positive (HR^+) and HER2-negative ($HER2^-$) breast cancer after menopause in combination with an aromatase inhibitor. Recently, the FDA expanded the indication for ribociclib to treat also pre/perimenopausal women with the above-mentioned subtypes of breast cancer.[2]

Ribociclib (Figure S1) is an orally bioavailable small molecule that binds to the ATP-binding cleft of CDK4/6, leading to the inhibition of these enzymes (IC_{50} 10 and 39 nM, respectively). After a dosage of 600 mg/day in the clinic, ribociclib is rapidly absorbed with a maximum plasma concentration between 1 and 5 h, and a half-life that ranges from 33 to 42 h. In addition to breast cancer, the efficacy of ribociclib to treat other malignancies including melanoma, nonsmall cell lung cancer, liposarcoma, glioblastoma, gynecologic cancers, prostate cancer, and others is currently investigated in clinical trials.[3,4]

Drug disposition and therefore drug efficacy can be affected by the drug efflux transporters P-glycoprotein (P-gp; MDR1; ABCB1) and Breast Cancer Resistance Protein (BCRP; ABCG2), which belong to the ATP-binding cassette (ABC) superfamily.[5] These efflux transporters are expressed in the apical membrane of organs with absorptive and eliminatory functions, like intestine, liver, and kidneys, as well as in various blood−tissue barriers, including the blood−brain barrier

Received: May 1, 2019
Revised: July 3, 2019
Accepted: July 22, 2019
Published: July 22, 2019

DOI: 10.1021/acs.molpharmaceut.9b00475
Mol. Pharmaceutics 2019, 16, 3842−3852

(BBB). Their function is to accelerate the elimination and limit the tissue penetration of xenobiotics, including drugs.[5,6] In addition, efficacy of transported anticancer agents can also be directly affected since both proteins can be expressed in some cancer cells. Indeed, several mechanisms involved in the upregulation of ABCB1 and/or ABCG2 in some cancer treatments have been described to be associated with multidrug resistance in breast cancer.[7−9]

Many anticancer agents are transport substrates of ABCB1 and/or ABCG2. Specifically within the CDK4/6 inhibitors, abemaciclib and palbociclib are substrates for human ABCB1 and mouse Abcg2, and for both compounds the penetration of the BBB improves when Abcb1a/1b is absent in rodents. For palbociclib, it was shown that its brain penetration is also restricted by mouse Abcg2.[10,11] According to the manufacturer, ribociclib is a weak substrate for ABCB1, but Sorf et al. showed that ribociclib is markedly transported by human ABCB1 *in vitro*.[12,13] However, the *in vivo* effects of the ABC efflux transporters on ribociclib disposition have not been described hitherto.

In preclinical studies in rats, ribociclib distributed extensively to most tissues except for the brain.[1] Because ABCB1 and ABCG2 are expressed at the BBB, they could potentially limit the brain accumulation of ribociclib. Breast cancer can often metastasize to the brain; therefore, it would be preferable to use an anticancer agent that can readily penetrate into the brain. As ribociclib is orally administered, ABCB1 and ABCG2 might also significantly impact on its oral bioavailability.

Similar to drug transporters, drug-metabolizing enzymes and their inter- and intraindividual variabilities can affect the therapeutic efficacy and safety of drugs since they can lead to deactivation, either directly or by facilitating its excretion from the body, or to bioactivation to form active and/or toxic compounds. In humans, CYP3A isoenzymes comprise the largest portion of cytochrome P450 (CYP450) enzymes in the liver, where CYP3A4 is the most abundant.[14,15] Ribociclib is mainly hepatically metabolized through CYP3A4. Three circulating metabolites of ribociclib have been reported, including M13 (*N*-hydroxylation), M4 (*N*-demethylation), and M1 (secondary glucuronide), but their contribution to the clinical activity is negligible.[3,12,16] In a drug−drug interaction study (DDI) it was found that the CYP3A inhibitor ritonavir could substantially increase the plasma exposure of ribociclib.[12,16]

In this study, we aimed to investigate the interaction of ribociclib with the efflux transporters ABCB1 and ABCG2 *in vitro* as well as *in vivo*, in order to assess their effects on oral bioavailability and tissue accumulation of ribociclib. We also studied the effect of coadministration of the ABCB1 and ABCG2 inhibitor elacridar. Finally, we determined to what extent ribociclib oral bioavailability and tissue accumulation is affected by CYP3A.

MATERIALS AND METHODS

Drugs. Ribociclib free base was purchased from Alsachim (Illkirch-Graffenstaden, France). Zosuquidar free base was supplied by Sequoia Research Products (Pangbourne, UK). Ko143 was obtained from Tocris Bioscience (Bristol, UK), and elacridar free base from Carbosynth Limited (Berkshire, UK).

***In Vitro* Transport Assays.** *Cell Culture.* Parental Madin−Darby Canine Kidney (MDCK-II) cells and subclones transduced with human hABCB1,[17,18] hABCG2,[19] and mouse mAbcg2[20] were cultured in DMEM glutamax (Gibco, Thermo Fisher Scientific, Waltham, MA), supplemented with 10% Fetal Bovine Serum F7524 (FBS, Sigma-Aldrich, Darmstadt, Germany) and 1% penicillin−streptomycin 10000 U/mL (Gibco) at 37°C in 5% CO_2. Cells were cultured for at least 2 weeks before the start of the transport assays, reaching a passage number of 15 for the parental, 10 for the hABCB1, 14 for the hABCG2, and 11 for the mAbcg2 cell line when seeded in the Transwell supports.

Transport Assays. Cell lines were seeded in 12-well Transwell permeable supports (Corning Life Sciences, Tewksbury, MA) using inserts with 12 mm internal diameter polycarbonate membrane (3 μm pore size), at a density of 2.5 × 10^5 cells per well. Cells were cultured for 3 days until a monolayer with tight junctions was formed. The tightness was evaluated by measuring the transepithelial electrical resistance (TEER). On day 3, cells were washed with Dulbecco's phosphate-buffered saline (DPBS, Gibco) prior to a 1 h preincubation with DMEM supplemented only with 10% FBS, and containing 5 μM zosuquidar (ABCB1 inhibitor) and/or 5 μM Ko143 (ABCG2 inhibitor), when appropriate. A concentration of 5 μM of the inhibitors was selected to ensure complete inhibition of even avid substrates of the respective ABC transporters. Thereafter, this medium was replaced with FBS-supplemented DMEM in the acceptor compartment, and with 5 μM ribociclib in FBS-supplemented DMEM in the donor compartment. For the inhibition experiments, the appropriate inhibitor(s) were added to both compartments. The total volume in each compartment was 0.75 mL for the apical and 1.5 mL for the basolateral side. Transport assays were independently performed in either the apical-to-basolateral (AB) or the basolateral-to-apical direction (BA). Transwell plates were incubated at 37 °C in 5% CO_2. At 1, 2, 4, and 8 h, 50 μL samples were taken from the acceptor compartment. Sample volumes were not replaced, and drug transport calculations were corrected for the change in volume and amount of removed drug. Monolayer integrity was assessed after the transport experiment by remeasuring the TEER. For all cell lines TEERs were above 95 Ohm·cm^2 before the start of the transport experiment, and they were not decreased when remeasured after 8 h at the end of the experiment. Inhibitor additions also did not negatively affect the TEER. Samples were stored at −20 °C until analysis.

Sample Measurement and Calculations. Ribociclib was quantified by liquid chromatography−tandem mass spectrometry (LC−MS/MS) using a modification of a previously described bioanalytical method.[21] A different concentration range was used (20 to 2500 ng/mL), and in order to maintain linearity within the new range, the collision energy in the MS detector was decreased to 35 V for ribociclib and the injection volume was reduced to 1 μL. Calibration standards and quality control samples were prepared in FBS-supplemented DMEM. $^2H_6$-ribociclib (AlsaChim) was used as an internal standard and added to each sample prior to sample pretreatment. Proteins were precipitated with acetonitrile, and after centrifugation (10 min, 23 100*g*), the supernatant was injected into the LC−MS/MS system. A partial validation was performed after these changes. Linearity, selectivity, accuracy, precision, lower limit of quantification (LLOQ), carry-over, dilution integrity, and stability were evaluated and found to be satisfactory according to international standards.[22,23]

The amount of ribociclib transported at each time point was calculated. Active transport due to efflux transporters was expressed by the efflux ratio (r), which is determined by the

DOI: 10.1021/acs.molpharmaceut.9b00475
Mol. Pharmaceutics 2019, 16, 3842−3852

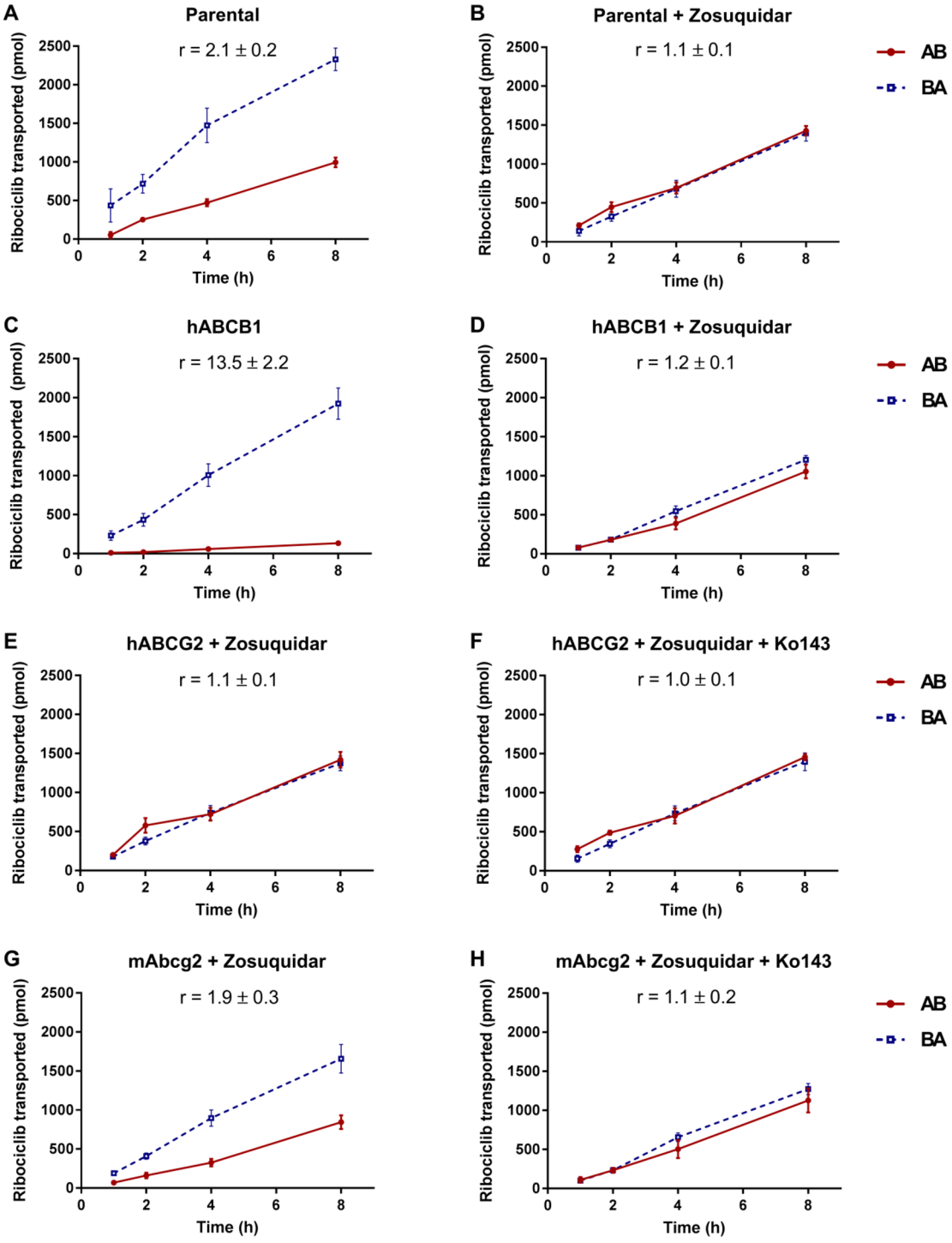

Figure 1. *In vitro* transport of ribociclib evaluated in MDCK-II cells either nontransduced (A, B) or transduced with human ABCB1 (C, D), human ABCG2 (E, F), or murine Abcg2 (G, H) cDNA. At $t = 0$, ribociclib (5 μM) was added in the donor compartment, either apical to assess apical-to-basolateral translocation, or basolateral to assess basolateral-to-apical transport. At 1, 2, 4, and 8 h, the concentration in the acceptor compartment was measured and plotted in the graphs as total transported amount ($n = 3$). D−H: zosuquidar was added to inhibit human and/or endogenous canine ABCB1. (F,H) Ko143 was added for the inhibition of human and murine ABCG2. r = efflux ratio. (red) Translocation from the apical to the basolateral compartment (AB). (blue) Translocation from the basolateral to apical compartment (BA). Data are presented as mean ± SD; 1000 pmol transport at 8 h corresponds to an approximate apparent permeability coefficient (P_{app}) of 6.2 × 10^{-6} cm/s.

apparent permeability coefficient (P_{app}) from basolateral-to-apical transported drug divided by the P_{app} from apical-to-basolateral translocated drug. A 1000 pmol transport at 8 h corresponds to an approximate apparent permeability coefficient (P_{app}) of 6.2 × 10^{-6} cm/s.

***In Vivo* Pharmacokinetics and Tissue Distribution of Ribociclib.** *Animals.* Female (FVB) WT, *Abcb1a/1b*$^{-/-}$,[24] *Abcg2*$^{-/-}$,[20] *Abc1a/1b*$^{-/-}$;*Abcg2*$^{-/-}$,[25] Cyp3a$^{-/-}$,[26] and Cyp3aXAV mice were used between 9 and 16 weeks of age. The homozygous CYP3A4-humanized transgenic mice (Cyp3aXAV, with CYP3A4 expression in both liver and intestine) were

DOI: 10.1021/acs.molpharmaceut.9b00475
Mol. Pharmaceutics 2019, 16, 3842−3852

generated by cross-breeding of transgenic mice with stable human CYP3A4 expression in liver or intestine, respectively, in a *Cyp3a*$^{-/-}$ background.[27] Animals were housed in a temperature-controlled environment with a 12 h light and 12 h dark cycle. Food (Transbreed, SDS Diets, Technilab-BMI, Someren, The Netherlands) and acidified water were provided *ad libitum*. Mice were housed and handled according to institutional guidelines complying with Dutch and EU legislation. All experiments were reviewed and approved by the institutional animal care and use committee.

Pharmacokinetic and Tissue Distribution Experiments. After at least 2 h of fasting, a dose of 20 mg/kg of ribociclib was orally administered, using a formulation containing 2 mg/mL of ribociclib in DMSO:Tween 80:10 mM HCl in water (5:5:90, v/v). Approximately 50 μL of blood was collected from the tip of the tail in heparin-coated microvette tubes (Sarstedt AG & Co., Nümbrecht, Germany) at 0.25, 0.5, 1, 3, and 8 h, or 0.25, 0.5, 1, 2, and 4 h, for the 24 and 8 h experiment, respectively. At either 8 or 24 h after administration, blood was collected by cardiac puncture under deep isoflurane anesthesia. The mice were then sacrificed by cervical dislocation and organs, including brain, liver, kidneys, spleen, and small intestine (cleaned from fecal content) were collected and weighed. Plasma was obtained from blood samples after 6 min centrifugation at 9000*g* and 4°C.

Tissue homogenates were prepared using the Fast Prep-24 5G homogenizer (MP Biomedicals Inc., Santa Ana, CA). For this, Bovine Serum Albumin (BSA, Fraction V), obtained from Roche Diagnostics GmbH (Mannheim, Germany), was dissolved at a concentration of 4% (w/v) in distilled water (B Braun Medical, Melsungen, Germany). Three milliliters of this solution was added to liver and small intestine, 2 mL to kidneys, and 1 mL to brain and spleen prior to the homogenization. All samples were stored at −20 or −70 °C until analysis.

Effect of Elacridar on Ribociclib Pharmacokinetics and Brain Accumulation. After at least 2 h of fasting, vehicle or 50 mg/kg of elacridar were orally administered (5 mg/mL of elacridar in DMSO-cremophor EL-water (1:2:7, v/v)) to WT and *Abcb1a/1b;Abcg2*$^{-/-}$ mice. Subsequently, after 15 min, 20 mg/kg of ribociclib was orally administered to each mouse. Blood samples were collected from the tip of the tail at 0.25, 0.5, 1, and 2 h. At the terminal time point (4 h), blood was collected by cardiac puncture under isoflurane anesthesia; brain and liver were collected and their homogenates were prepared as described above.

Ribociclib Quantification, Pharmacokinetic Calculation, and Statistics. Ribociclib concentrations in plasma and tissue homogenates were determined using the previously described LC−MS/MS bioanalytical method.[21]

All pharmacokinetic parameters were calculated with a noncompartmental model using the add-in PKSolver program in Microsoft Excel.[28] In addition to ribociclib concentration in tissues, tissue-to-plasma ratios and tissue accumulation of ribociclib were calculated by dividing by plasma concentration at the terminal time-point, and by the area under the plasma concentration−time curve ($AUC_{0\text{-}t}$), respectively. Statistical analysis was done using the software GraphPad Prism 7 (GraphPad software, San Diego, CA). All data were log-transformed before statistical analysis. Student's t and one-way ANOVA statistical tests were applied when two and multiple groups were compared, respectively. The Bonferroni posthoc test was used for multiple comparisons. Differences were considered statistically significant when $P < 0.05$.

RESULTS

***In Vitro* Transport of Ribociclib.** To determine whether and to what extent ribociclib is a transport substrate of ABCB1 and ABCG2, an *in vitro* transwell assay was performed using the polarized parental Madin−Darby Canine Kidney (MCDK-II) cell line and subclones overexpressing hABCB1, hABCG2, and mAbcg2. In the parental MCDK-II cell line, ribociclib (added at 5 μM) was modestly transported to the apical side (efflux ratio $r = 2.1$, Figure 1A). This transport was completely inhibited by the ABCB1 inhibitor zosuquidar ($r = 1.1$, Figure 1B). This suggests that the ribociclib transport was due to the low-level endogenous canine ABCB1 known to be expressed in the parental MDCK-II cell line.[29] In the MDCK-II-hABCB1 cells, ribociclib was strongly transported to the apical side ($r = 13.5$, Figure 1C), and this transport was completely inhibited by zosuquidar ($r = 1.2$, Figure 1D). In transport experiments performed with MDCK-II-hABCG2 and MDCK-II-mAbcg2 cells, zosuquidar was added to inhibit the background activity of the endogenous canine ABCB1. In the hABCG2-transduced cell line, ribociclib was not noticeably actively transported to the apical side since translocation rates in both directions were similar. Furthermore, the efflux ratios without and with the ABCG2 inhibitor Ko143 were comparable (1.1 and 1.0, respectively, Figure 1E,F). However, ribociclib was modestly transported in the apical direction in the MDCK-II-mAbcg2 cell line ($r = 1.9$), and Ko143 inhibited this transport completely ($r = 1.1$) (Figure 1G,H). Ribociclib thus appears to be a very good transport substrate of hABCB1, whereas it is not noticeably transported by hABCG2 and only modestly by mAbcg2 *in vitro*.

Effect of ABCB1 and ABCG2 on Ribociclib Pharmacokinetics and Tissue Distribution in Mice. Based on the *in vitro* transport results, we evaluated a possible effect of both transporters on ribociclib plasma pharmacokinetics (oral bioavailability) and tissue distribution. A 24 h pilot experiment was performed in WT and *Abcb1a/1b*$^{-/-}$*;Abcg2*$^{-/-}$ mice. Since ribociclib is prescribed to treat breast cancer, which mostly occurs in women, female mice were used. Ribociclib was orally administered at 20 mg/kg, resulting in similar plasma concentrations as seen in patients after a single oral dose of 600 mg.[30,31] As shown in Figure 2, in the absence of *Abcb1a/1b* and *Abcg2*, the area under the plasma concentration−time curve (AUC) significantly increased by 2.3-fold compared to

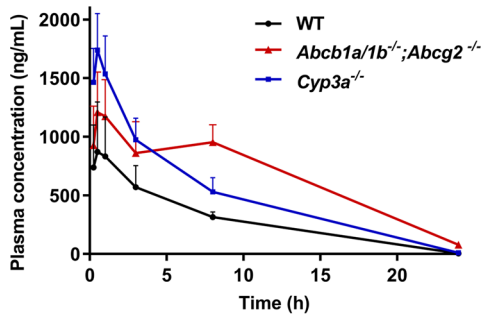

Figure 2. Plasma concentration−time curves of ribociclib over 24 h in female WT, *Abcb1a/1b*$^{-/-}$*;Abcg2*$^{-/-}$, and *Cyp3a* $^{-/-}$ mice after oral administration of 20 mg/kg. Data are presented as mean ± SD ($n = 6$).

DOI: 10.1021/acs.molpharmaceut.9b00475
Mol. Pharmaceutics 2019, 16, 3842−3852

WT mice ($P < 0.001$, Table 1). Furthermore, ribociclib showed a slower elimination in *Abcb1a/1b*$^{-/-}$;*Abcg2*$^{-/-}$ mice compared to WT mice, especially beyond 3 and 8 h after oral administration, which is reflected in the increase in the plasma concentration at 24 h (Figure S2). However, the maximum plasma concentration (C_{max}) of ribociclib and the time to reach it (T_{max}) were not significantly different between the two mouse strains (Table 1, $P > 0.05$).

Table 1. Pharmacokinetic Parameters 24 h after Oral Administration of 20 mg/kg Ribociclib to Female WT, *Abcb1a/1b*$^{-/-}$;*Abcg2*$^{-/-}$, and *Cyp3a*$^{-/-}$ Mice[a]

	genotype		
parameter	WT	*Abcb1a/1b*$^{-/-}$;*Abcg2*$^{-/-}$	*Cyp3a*$^{-/-}$
AUC_{0-24h} (h·ng/mL)	6885 ± 1215	15775 ± 2515***	11967 ± 2427**
fold change AUC_{0-24h}	1.0	2.3	1.7
T_{max} (h)	0.5−1.0	0.5−8.0	0.5
C_{max} (ng/mL)	1036 ± 352	1308 ± 226	1739 ± 127**
C_{brain} (ng/g)	3.3 ± 0.5	1690 ± 668***	5.4 ± 1.6**
$K_{p,brain}$	0.70 ± 0.19	24.8 ± 7.9***	0.67 ± 0.15
fold increase $K_{p,brain}$	1.0	35.5	1.0
P_{brain} ($\times 10^{-3}$ h^{-1})	0.5 ± 0.2	108.2 ± 32.3***	0.5 ± 0.3

[a]Data are presented as mean ± SD, except for T_{max} (n = 5−6). AUC_{0-24h}, area under the plasma concentration−time curve; C_{max}, maximum concentration in plasma; T_{max}, time point (h) of maximum plasma concentration; C_{brain}, brain concentration; $K_{p,brain}$, brain-to-plasma ratio; P_{brain}, brain accumulation, calculated by determining the ribociclib brain concentration at 24 h relative to the AUC_{0-24h}. Data were log-transformed for statistical analysis. **, $P < 0.01$; ***, $P < 0.001$ compared to WT mice. Cyp3a data were treated separately for statistical analysis.

Ribociclib was also quantified in brain, liver, kidney, spleen, and small intestine tissue 24 h after oral administration. Interestingly, the brain concentration of ribociclib was vastly increased in the *Abcb1a/1b*$^{-/-}$;*Abcg2*$^{-/-}$ mice. This increase was not only dependent on the higher plasma concentration in this strain since the brain-to-plasma ratio ($K_{p,brain}$) was also dramatically increased by around 30-fold ($P < 0.001$, Figure 3A−C, Table 1). In other organs like liver, ribociclib concentrations were also significantly increased in *Abcb1a/1b*$^{-/-}$;*Abcg2*$^{-/-}$ compared to WT mice. However, this increase was primarily associated with the higher ribociclib plasma concentration at the terminal time point since there was no difference between both strains after correction for the plasma concentration (Figure 3D−F, Figure S3). For kidneys and spleen, the organ-to-plasma ratios in *Abcb1a/1b*$^{-/-}$;*Abcg2*$^{-/-}$ mice were moderately lower than in WT mice, whereas the tissue accumulations were moderately higher, suggesting that the difference may have been primarily caused by the substantial difference in plasma concentration between the strains at 24 h (Figure S3). In general, ribociclib was highly distributed in organs compared to plasma since all tested organ-to-plasma ratios showed a mean higher than 25 in WT

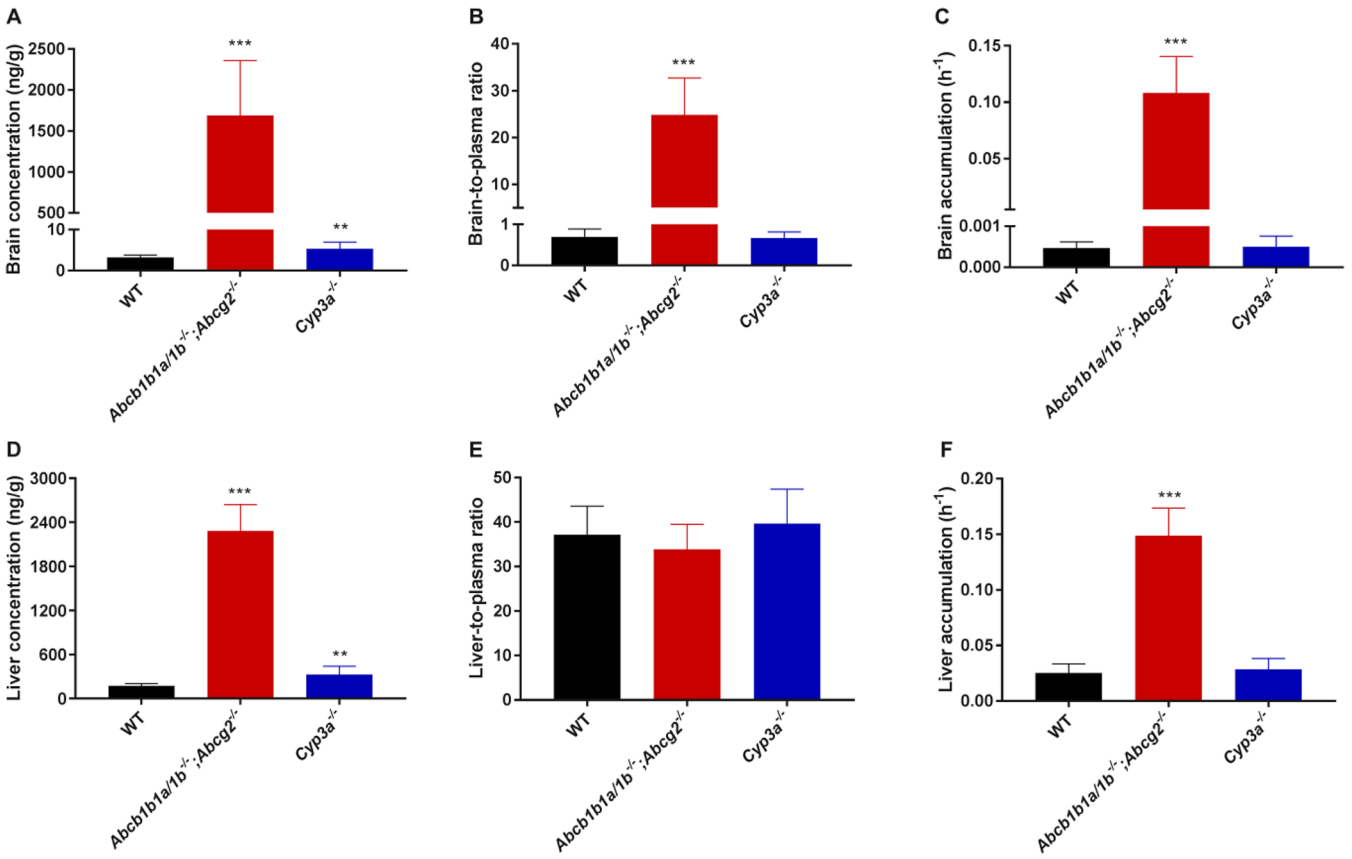

Figure 3. Brain and liver concentration (A,D), tissue-to-plasma ratio (B,E), and tissue accumulation (C,F) of ribociclib in WT, *Abcb1a/1b*$^{-/-}$;*Abcg2*$^{-/-}$, and *Cyp3a*$^{-/-}$ mice 24 h after oral administration of 20 mg/kg of ribociclib. Data are presented as mean ± SD (n = 6). **, $P < 0.01$; ***, $P < 0.001$ compared to WT mice.

DOI: 10.1021/acs.molpharmaceut.9b00475
Mol. Pharmaceutics 2019, 16, 3842−3852

mice except for the brain, where the ratio was just below 1 (Table 1, Figure 3, Figure S3).

To further investigate the single and combined effects of these transporters on plasma pharmacokinetics and tissue distribution of ribociclib, we performed a second experiment with oral ribociclib at 20 mg/kg, which was terminated at 8 h, when ribociclib plasma concentrations were still relatively high. In addition to WT and *Abcb1a/1b*$^{-/-}$;*Abcg2*$^{-/-}$ mice, also single *Abcb1a/1b*$^{-/-}$ and *Abcg2*$^{-/-}$ mouse strains were included. As shown in Figure 4A and Table 2, the ribociclib plasma AUC_{0-8h} was not significantly different among the mouse strains ($P > 0.05$). Most other pharmacokinetic parameters were not significantly different either. However, the elimination from 1 h on was slower when Abcb1a/1b was absent in both the *Abcb1a/1b*$^{-/-}$ and especially the *Abcb1a/1b;Abcg2*$^{-/-}$ mice (Figure S4A), which is consistent with what we observed in the pilot experiment, albeit a bit less pronounced. Thus, Abcb1a/1b may be an important factor for the intermediate and late elimination phases of ribociclib.

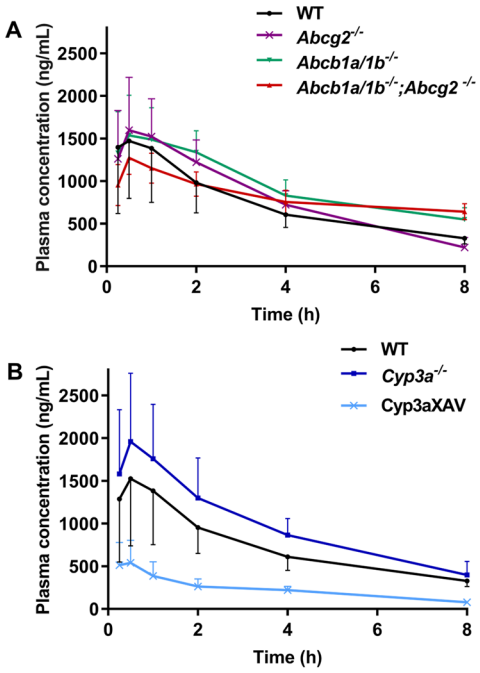

Figure 4. Plasma concentration−time curves of ribociclib over 8 h in female WT, *Abcg2*$^{-/-}$, *Abcb1a/1b*$^{-/-}$, and *Abcb1a/1b*$^{-/-}$;*Abcg2*$^{-/-}$ (A), and female WT, *Cyp3a*$^{-/-}$, and Cyp3aXAV (B) mice after oral administration of 20 mg/kg ribociclib. Data are presented as mean ± SD (n = 6−8).

The ABC efflux transporters further had a profound effect at 8 h on the brain accumulation of ribociclib, but not in the other organs (Figure 5, Figure S5). The brain-to-plasma ratio was increased by 26-fold ($P < 0.001$, Table 2, Figure 5A−C) in the absence of Abcb1a/1b and Abcg2. Similarly, in the single *Abcb1a/1b*$^{-/-}$ mice, the brain-to-plasma ratio was increased by 30-fold ($P < 0.001$, Table 2). In contrast, single *Abcg2*$^{-/-}$ mice did not demonstrate any effect on brain accumulation since the brain-to-plasma ratio was comparable to that in WT mice ($P > 0.05$, Table 2, Figure 5A−C). These results suggest that the brain accumulation of ribociclib is extensively limited by Abcb1a/1b in the BBB, whereas Abcg2 does not have a significant effect. This is further supported by the lack of significant differences between *Abcb1a/1b*$^{-/-}$ and *Abcb1a/1b*$^{-/-}$;*Abcg2*$^{-/-}$ mice (Figure 5B,C).

Effect of CYP3A on Ribociclib Pharmacokinetics and Tissue Distribution in Mice. To investigate the interaction between ribociclib and murine Cyp3a, a 24 h oral ribociclib (20 mg/kg) pilot experiment was performed, where the pharmacokinetics between WT and the *Cyp3a*$^{-/-}$ mice were compared. As shown in Figure 2 and Table 1, when Cyp3a was knocked out, the plasma AUC and C_{max} of ribociclib significantly increased by 1.7-fold ($P < 0.01$), but the T_{max} was similar. These results suggest that mCyp3a-mediated metabolism significantly limits ribociclib plasma exposure. The tissue distribution of ribociclib between both strains was also compared, but no relevant differences between the two groups were evident considering the higher plasma exposure in *Cyp3a*$^{-/-}$ mice (Figure 3 and Supplementary Figure S3).

To study the possible *in vivo* impact of human CYP3A4, a transgenic mouse strain with expression of human CYP3A4 in liver and small intestine in a *Cyp3a*$^{-/-}$ background (Cyp3aXAV mice) was included in a subsequent 8-h experiment. Ribociclib pharmacokinetics and tissue distribution were compared among the three mouse genotypes over 8 h after oral administration of ribociclib at 20 mg/kg. Plasma exposure of ribociclib decreased markedly in the Cyp3aXAV

Table 2. Pharmacokinetic Parameters 8 h after Oral Administration of 20 mg/kg Ribociclib to Female WT, *Abcb1a/1b*$^{-/-}$, *Abcg2*$^{-/-}$, *Abcb1a/1b*$^{-/-}$;*Abcg2*$^{-/-}$, *Cyp3a*$^{-/-}$, and Cyp3aXAV Mice[a]

	genotype					
parameter	WT	*Abcg2*$^{-/-}$	*Abcb1a/1b*$^{-/-}$	*Abcb1a/1b*$^{-/-}$;*Abcg2*$^{-/-}$	*Cyp3a*$^{-/-}$	Cyp3aXAV
AUC_{0-8h} (h·ng/mL)	5901 ± 1760	6496 ± 1480	7616 ± 1014	6576 ± 719	7021 ± 2586	1834 ± 490$^{\#\#\#}$
fold change AUC_{0-8h}	1.0	1.1	1.3	1.1	1.2	0.31
T_{max} (h)	0.25−2	0.5−1	0.5−2	0.5−2	0.5−1	0.25−0.5
C_{max} (ng/mL)	1774 ± 833	1659 ± 551	1565 ± 441	1288 ± 182	1963 ± 791	546 ± 260$^{\#\#\#}$
C_{brain} (ng/g)	80.4 ± 28.2	76.1 ± 19.6	4066 ± 888***	4181 ± 672***	77.4 ± 17.0	27.1 ± 8.4$^{\#\#\#}$
$K_{p,brain}$	0.25 ± 0.09	0.40 ± 0.15	7.83 ± 2.55***	6.57 ± 0.70***	0.23 ± 0.07	0.35 ± 0.15
fold increase $K_{p,brain}$	1.0	1.6	31.2	26.4	0.9	1.4
P_{brain} (× 10^{-3} h^{-1})	14.1 ± 3.6	12.3 ± 3.6	535 ± 95***	635 ± 70***	10.6 ± 4.6	15.3 ± 5.2

[a]Data are presented as mean ± SD, except for T_{max} (n = 6−8). AUC_{0-8h}, area under the plasma concentration−time curve; C_{max}, maximum concentration in plasma; T_{max}, time point (h) of maximum plasma concentration; C_{brain}, brain concentration; $K_{p,brain}$, brain-to-plasma ratio; P_{brain}, brain accumulation, calculated by determining the ribociclib brain concentration at 8 h relative to the AUC_{0-24h}. Data were log-transformed for statistical analysis. ***, $P < 0.001$ compared to WT mice. $^{\#\#\#}$, $P < 0.001$ compared to *Cyp3a*$^{-/-}$ mice. CYP3A groups were treated separately for the statistical analysis.

DOI: 10.1021/acs.molpharmaceut.9b00475
Mol. Pharmaceutics 2019, 16, 3842−3852

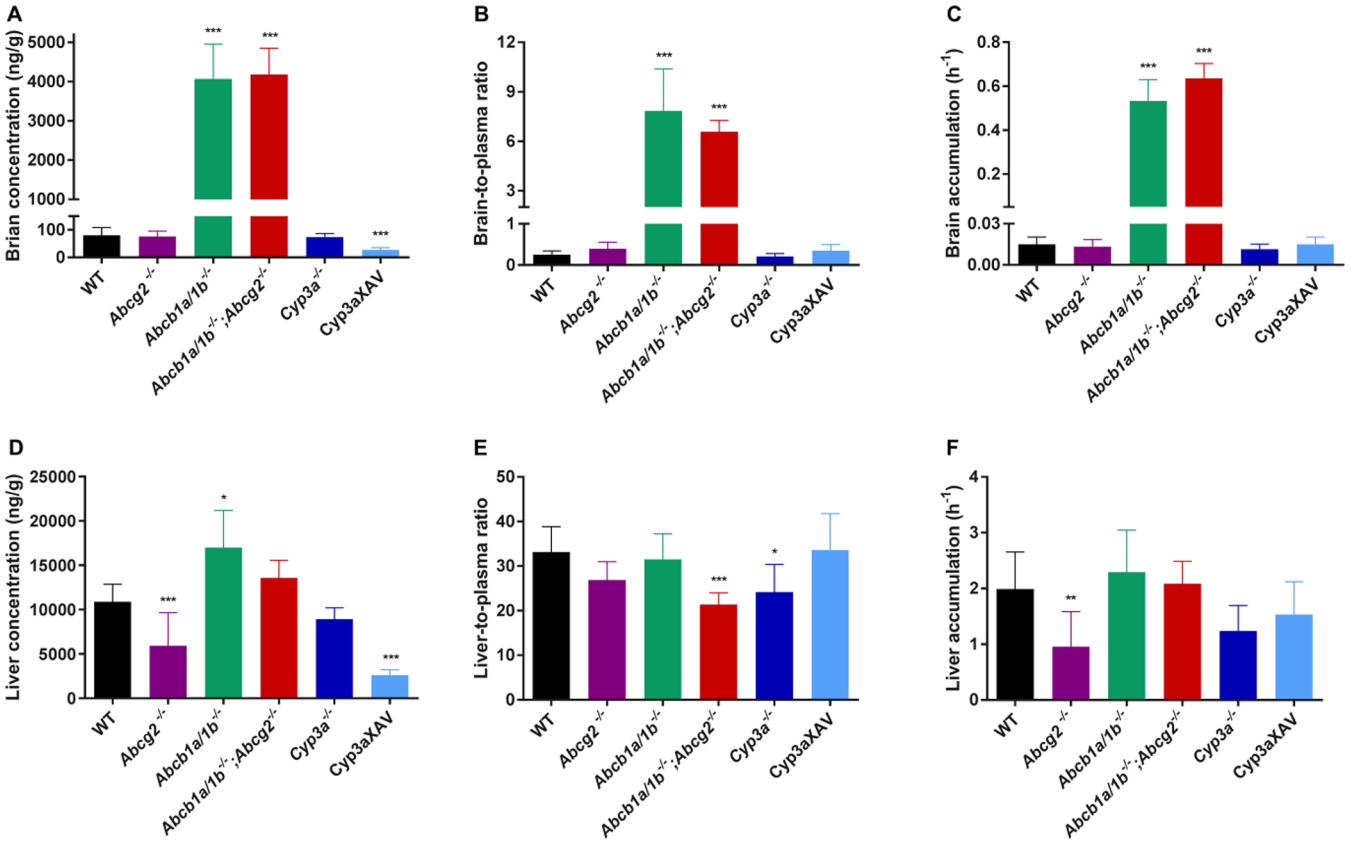

Figure 5. Brain and liver concentration (A,D), tissue-to-plasma ratio (B,E), and tissue accumulation (C,F) of ribociclib in WT, *Abcb1a/1b*$^{-/-}$, *Abcg2*$^{-/-}$, *Abcb1a/1b*$^{-/-}$;*Abcg2*$^{-/-}$, *Cyp3a*$^{-/-}$, and Cyp3aXAV mice 8 h after oral administration of 20 mg/kg of ribociclib. Data are presented as mean ± SD (n = 6–8). *, P < 0.05; **, P < 0.01; ***, P < 0.001 compared to WT mice.

Table 3. Effect of Elacridar on Pharmacokinetic Parameters 4 h after Oral Administration of 20 mg/kg Ribociclib to Female WT and *Abcb1a/1b*$^{-/-}$;*Abcg2*$^{-/-}$ Mice[q]

	genotype			
	vehicle		elacridar	
parameter	WT	*Abcb1a/1b*$^{-/-}$;*Abcg2*$^{-/-}$	WT	*Abcb1a/1b*$^{-/-}$;*Abcg2*$^{-/-}$
AUC_{0-4h} (h·ng/mL)	2134 ± 273	3305 ± 436	4804 ± 1695***	2976 ± 636
fold change AUC_{0-4h}	1.0	1.5	2.3	1.4
T_{max} (h)	0.25–1	0.5–2	0.25–0.5	0.25–2
C_{max} (ng/mL)	809 ± 119	1129 ± 114	2132 ± 1191**	1134 ± 350
C_{brain} (ng/g)	69.1 ± 15.7	3430 ± 557***	3945 ± 890***	2965 ± 1163***
$K_{p,brain}$	0.25 ± 0.07	6.88 ± 1.40***	6.34 ± 0.86***	5.80 ± 1.30***
fold increase $K_{p,brain}$	1.0	27.5	24.9	23.2
P_{brain} ($\times 10^{-3}$ h^{-1})	32.7 ± 7.8	1043 ± 165***	894 ± 244***	934 ± 207***

[q]Data are presented as mean ± SD, except for T_{max} (n = 6). AUC_{0-4h}, area under the plasma concentration–time curve; C_{max}, maximum concentration in plasma; T_{max}, time point (h) of maximum plasma concentration; C_{brain}, brain concentration; $K_{p,brain}$, brain-to-plasma ratio; P_{brain}, brain accumulation, calculated by determining the ribociclib brain concentration at 4 h relative to the AUC_{0-4h}. Data were log-transformed for statistical analysis. **, P < 0.01; ***, P < 0.001 compared to vehicle-treated WT mice.

mice compared to *Cyp3a*$^{-/-}$ mice, with a 3.8-fold reduced plasma AUC_{0-8h} (P < 0.001, Figure 4B, Table 2). In addition, the ribociclib C_{max} significantly decreased by around 70% in the CYP3aXAV mice (P < 0.001, Table 2). Also, in this experiment the plasma AUC was somewhat higher in *Cyp3a*$^{-/-}$ than in WT mice, but the difference was not significant. There was again no meaningful difference in organ exposure among the three strains considering the differences in plasma exposure (Figure 5, Figure S5). These results support that ribociclib is extensively metabolized *in vivo* via human CYP3A4, resulting in reduced systemic exposure, but without a strong effect on tissue distribution of the drug.

Effect of Elacridar on Ribociclib Oral Bioavailability and Brain Accumulation. Since the brain accumulation of ribociclib was strongly affected by Abcb1a/1b, we investigated whether coadministration of elacridar, a dual inhibitor for ABCB1 and ABCG2, could enhance the ribociclib brain accumulation. Elacridar (50 mg/kg) or vehicle was orally administered 15 min prior to the administration of ribociclib (20 mg/kg) to WT and *Abcb1a/1b;Abcg2*$^{-/-}$ mice. In order to optimally assess the effects of elacridar, the experiment was

DOI: 10.1021/acs.molpharmaceut.9b00475
Mol. Pharmaceutics 2019, 16, 3842–3852

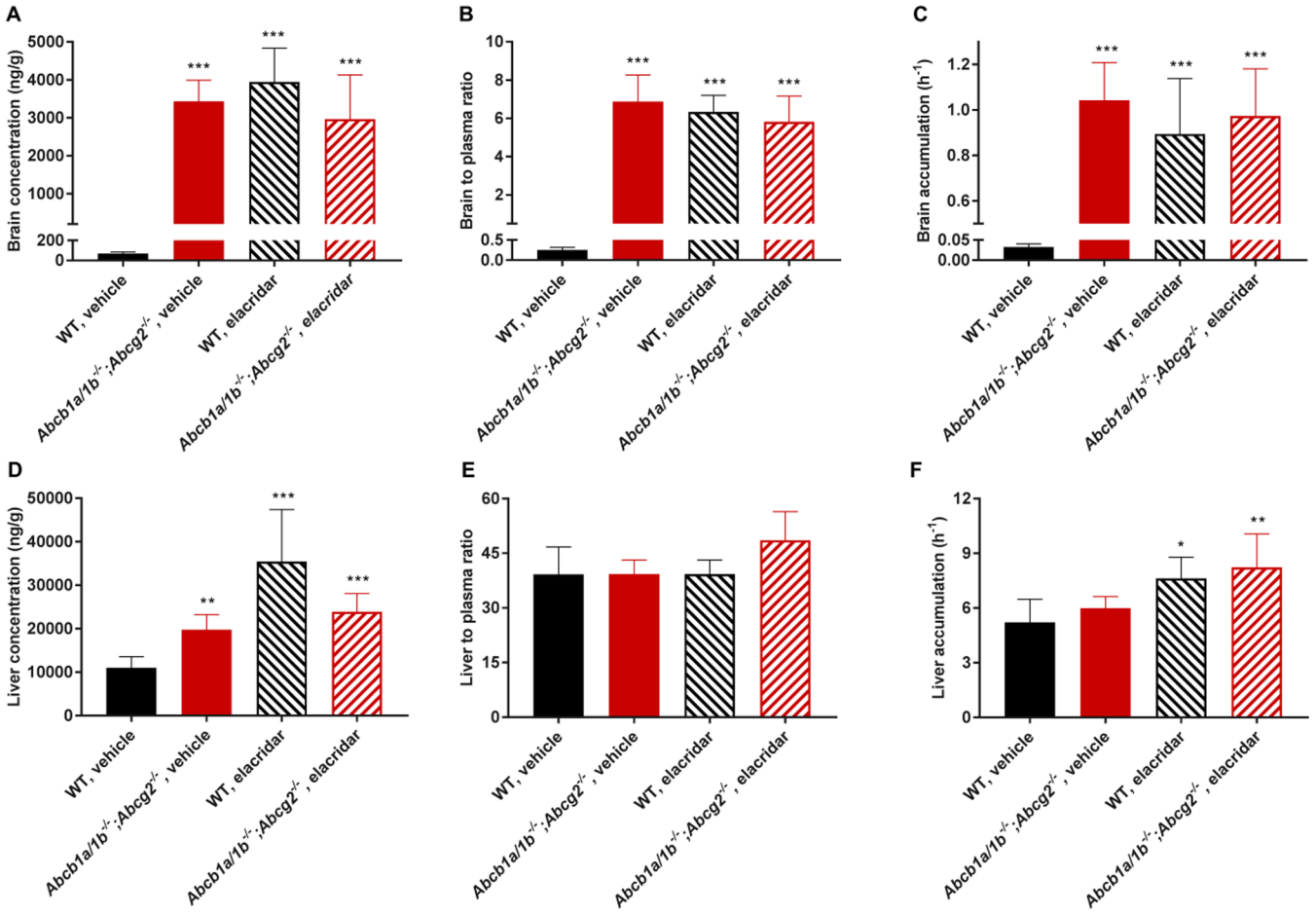

Figure 6. Brain and liver concentration (A,D), brain-to-plasma ratio (B,E), and brain accumulation (C,F) of ribociclib in WT and *Abcb1a/1b*$^{-/-}$;*Abcg2*$^{-/-}$ mice 4 h after oral administration of 20 mg/kg of ribociclib with oral vehicle or elacridar coadministration (50 mg/kg). Data are presented as mean ± SD (n = 5−6). *, P < 0.05; **, P < 0.01; ***, P < 0.001 compared to vehicle-treated WT mice.

terminated at 4 h, which is around the reported median T_{max} of elacridar in mice receiving a similar oral elacridar dose,[32] and while ribociclib plasma concentrations were still high. The plasma AUC_{0-4h} and the C_{max} were, respectively, 2.3-fold and 2.6-fold higher in WT mice treated with elacridar compared to WT mice treated with vehicle (P < 0.001, Table 3, Figure S6). High interindividual variation was observed in the WT mice treated with elacridar compared to other groups, especially during the first 2 h. This may perhaps be explained by interindividual variation in the elacridar exposure of the Abcb1a/1b and Abcg2 transporters.

Strong evidence of full Abcb1a/1b inhibition by elacridar at the BBB was found (Figure 6A−C, Table 3). In the vehicle-treated groups, the brain-to-plasma ratio at 4 h was 28-fold higher in *Abcb1a/1b;Abcg2*$^{-/-}$ compared to WT mice (P < 0.001, Table 3), similar to the results found at 8 and 24 h. In elacridar-treated WT mice, the brain-to-plasma ratio dramatically increased by 25-fold compared to the vehicle-treated group (P < 0.001, Table 3, Figure 6B). This value was essentially the same as that in vehicle- or elacridar-treated *Abcb1a/1b;Abcg2*$^{-/-}$ mice (P > 0.05, Table 3, Figure 6B). This indicates that elacridar could completely inhibit Abcb1a/1b in the BBB. Moreover, since the brain-to-plasma ratios were not significantly different between the *Abcb1a/1b;Abcg2*$^{-/-}$ vehicle and elacridar groups, it appears that the elacridar effect was specifically due to the inhibition of mAbcb1a/1b and not due to interaction with other systems. In the liver, elacridar coadministration with ribociclib did not cause significant changes in the tissue-to-plasma ratios in either WT or *Abcb1a/1b;Abcg2*$^{-/-}$ mice (P > 0.05, Figure 6E).

DISCUSSION

In this study we show that ribociclib is a good transport substrate of hABCB1 but not noticeably of hABCG2 and a poor substrate of mAbcg2 *in vitro*. *In vivo* only mAbcb1a/1b had a significant impact on ribociclib pharmacokinetics and tissue distribution in mice. The oral bioavailability of ribociclib was significantly affected by the absence of Abcb1a/1b and Abcg2, increasing the AUC_{0-24h} by 2.3-fold. Ribociclib brain accumulation was drastically increased (at least 23-fold) when Abcb1a/1b was knocked out, demonstrating that this transporter plays an important role in the BBB in limiting the brain penetration of ribociclib. In contrast, ribociclib distribution to liver, kidneys, spleen, and small intestine was not markedly affected by Abcb1a/1b and Abcg2. We further showed that elacridar coadministration can completely inhibit Abcb1a/1b activity at the BBB, dramatically enhancing the brain accumulation of ribociclib. Oral bioavailability of ribociclib was further extensively affected by transgenic human CYP3A4, decreasing the AUC_{0-8h} by 3.8-fold, in line with extensive ribociclib metabolism by human CYP3A4.

DOI: 10.1021/acs.molpharmaceut.9b00475
Mol. Pharmaceutics 2019, 16, 3842−3852

As the present study was nearing completion, Sorf et al. showed that ribociclib is a transport substrate of hABCB1 but not of hABCG2.[13] These results are consistent with our data, but they contrast with the FDA and EMA documentation stating that ribociclib is a weak substrate of ABCB1, which is therefore unlikely to affect ribociclib exposure.[12,16] We also evaluated the transport in mouse Abcg2 overexpressing cells where the efflux transport was 1.9. According to the International Transporter Consortium, since the efflux ratio is <2, ribociclib is considered a poor or non-Abcg2 substrate.[5] For ribociclib, this consideration was reflected in our *in vivo* results, where only Abcb1a/1b had an impact on ribociclib plasma pharmacokinetics and tissue distribution, whereas mouse Abcg2 did not have any noticeable effect. It is thus very unlikely that hABCG2 will have a noticeable impact on human ribociclib pharmacokinetics and tissue distribution.

Our results suggest that Abcb1a/1b primarily has an impact on the elimination of ribociclib, which was slower when this transporter was absent (Figures S1 and S3), significantly increasing the ribociclib AUC_{0-24h} by 2.3-fold ($P < 0.001$, Table 1, Figure 2). This effect was clear beyond 4 and 8 h, but at earlier time points, this effect was not evident. This may partly explain why only the plasma AUC_{0-24h} was significantly affected and not the AUC_{0-8h} and AUC_{0-4h}. Ribociclib is mostly excreted via feces, where unchanged ribociclib amounts have been reported from 10.2% (in beagle dogs) to 17.3% (in humans) of the dose, and to a lesser extent in urine (12.1% in humans).[12,16] Based on our data, we speculate that Abcb1a/1b could mediate hepatobiliary excretion and/or direct intestinal excretion of ribociclib, or reduce its intestinal reuptake when the intestinal luminal concentration is relatively low. Each of these processes, or a combination thereof, could explain the delayed elimination of ribociclib that we observed in the absence of Abcb1a/1b.

The most striking finding was that Abcb1a/1b was responsible for limiting the ribociclib brain accumulation. So far, the penetration of ribociclib into the central nervous system (CNS) has not been fully characterized, and there is controversial information about the ability of ribociclib to penetrate into the brain.[33,34] Although, according to the FDA and EMA information, ribociclib showed a low or absent brain penetration in rats,[12,16] Patel et al. reported that ribociclib penetrates into the CNS in mouse models especially in brain tumors.[35] It is worth noting that the BBB or blood−tumor barrier (BTB) is often partly disturbed in brain metastases of breast cancer mouse models, resulting in variably increased drug levels and passive permeability in the metastases.[36,37] However, variation in permeability is high, and the BTB is rarely completely disrupted. Consequently, only ∼10% of brain metastases is expected to be leaky enough to allow efficacious drug concentrations of conventional chemotherapeutics into the lesions. Additional measures to further enhance permeability of the BBB and BTB might therefore improve therapy responses. In the present study we found that in the WT situation, the brain-to-plasma ratio was 0.25 at 4 and 8 h after oral administration of 20 mg/kg of ribociclib (Tables 2 and 3). Therefore, ribociclib is able to significantly cross the BBB even in WT mice, but its penetration to the brain is still dramatically limited by Abcb1a/1b.

The high efflux ratio in ABCB1-overexpressing cells *in vitro* correlates well with the *in vivo* role of Abcb1a/1b in the BBB. This implies that also in the human situation ABCB1 activity may limit ribociclib penetration into the brain. There is a lot of interest in ribociclib brain penetration since clinical investigation in pediatric patients with neuroblastoma or malignant rhabdoid tumors showed that ribociclib displayed preliminary signs of brain tumor stabilization.[38,39] Currently, several phase I/II clinical trials are ongoing to investigate the efficacy of ribociclib in brain tumors either alone or in combination with everolimus.[33] In addition, drugs that cross the BBB are needed since metastatic brain tumors are the most common type of brain tumors, occurring in approximately 20 to 40% of cancer patients.[10,40] Interestingly, the incidence of such metastases is rising due to several factors, including the improved therapeutic efficacy of many modern targeted drugs against tumors occurring outside of the CNS.[10,40,41] Among metastatic brain tumors, breast cancer presents the second highest frequency in brain metastasis, just after lung cancer.[10,40,41] Here, we also showed that the coadministration of 50 mg/kg of elacridar with ribociclib completely inhibits Abcb1a/1b in the BBB, increasing the brain penetration to the same extent as when Abcb1a/1b was ablated. Therefore, the efficacy of ribociclib to treat (metastatic) brain tumors in the clinic could potentially be enhanced by inhibiting hABCB1 since we have shown that ribociclib is also highly transported by hABCB1. Furthermore, since cancer cells themselves also often express ABCB1, they can be intrinsically resistant to ribociclib therapy, and ABCB1 inhibitors (like elacridar) could be coadministered to improve the efficacy of ribociclib against such tumors.

Overlap in substrate specificities has been observed between CYP enzymes and the ABC transporters, which has led to the idea that they may work synergistically to promote drug elimination.[42] Our CYP3A studies show that ribociclib is eliminated by both mouse Cyp3a and human CYP3A4. Oral bioavailability of ribociclib is affected by these metabolic enzymes but to different extents; while in the *Cyp3a*$^{-/-}$ mice, the plasma AUC was barely affected, in the CYP3A4 transgenic mice, the AUC was strongly decreased. The modest difference in AUCs between *Cyp3a*$^{-/-}$ and WT mice suggests that the contribution of mouse Cyp3a to the ribociclib metabolism is minor, and hence, ribociclib metabolism in mice could be accomplished also by other enzymes. Ribociclib was primarily metabolized by CYP3A4/5 (approximately 78%) and Flavin-containing monooxygenase 3 (FMO3, approximately 20%) *in vitro*, whereas *in vivo* studies in rats showed that the metabolism was dominated by direct phase II sulfation.[12,16] Probably also in *Cyp3a*$^{-/-}$ mice, some of these non-CYP3A enzymes could take over ribociclib metabolism. In contrast, the human CYP3A4 markedly limited the oral bioavailability of ribociclib, decreasing the AUC_{0-8h} by 3.8-fold. This suggests that hepatic and intestinal CYP3A4 contributes to a high extent to the first-pass metabolism of ribociclib. The overall effect of transgenic CYP3A4 in our mouse models (3.8-fold decrease in AUC) was similar to the ritonavir effect found in humans (3.2-fold increase in AUC) when ritonavir was coadministered with ribociclib. Our results thus further support that, in the human situation, ribociclib is extensively metabolized via CYP3A4 and its oral bioavailability is strongly restricted by this enzyme. CYP3A4 has a wide substrate specificity, and it can be strongly inhibited and/or induced by many different drugs and food components. Furthermore, genetic polymorphisms can also markedly affect its activity. All these factors might potentially contribute to high levels of variation in CYP3A4 activity, which may impact on oral bioavailability; thus, plasma concentrations of ribociclib should

DOI: 10.1021/acs.molpharmaceut.9b00475
Mol. Pharmaceutics 2019, 16, 3842−3852

be carefully monitored in patients to ensure optimal therapeutic exposure.[14,15]

CONCLUSION

This study shows that ribociclib is avidly transported by ABCB1. This transporter dramatically restricts the brain penetration of ribociclib *in vivo*, whereas it does not considerably affect the relative ribociclib distribution in other tissues. Our results further suggest that ABCB1 can play a significant role in ribociclib elimination. In contrast, ABCG2 does not have any noticeable effect on ribociclib plasma pharmacokinetics and tissue distribution. Moreover, coadministration of elacridar can completely inhibit the activity of ABCB1 at the BBB, dramatically improving the brain penetration of ribociclib. Our experiments also support that the oral bioavailability of ribociclib is markedly limited by human CYP3A4 activity, but this does not affect the relative tissue distribution. The risk of high variation in oral exposure due to variable CYP3A4 activity must thus be considered while using ribociclib in patients. The insights gained from this study may be useful to further improve the efficacy of ribociclib in the clinic, especially for the treatment of (metastatic) brain tumors.

ASSOCIATED CONTENT

Supporting Information

The Supporting Information is available free of charge on the ACS Publications website at DOI: 10.1021/acs.molpharmaceut.9b00475.

Chemical structure of ribociclib; (semilog) plasma concentration−time curves of ribociclib in the different mouse strains; kidney, spleen, and small intestine concentrations of ribociclib; tissue-to-plasma ratios and relative tissue accumulation at 24 and 8 h after oral administration (PDF)

AUTHOR INFORMATION

Corresponding Author

*Mailing Address: Division of Pharmacology Antoni van Leeuwenhoek, The Netherlands Cancer Institute Plesmanlaan 121, 1066 CX Amsterdam, The Netherlands. Tel: +31205122046. E-mail: a.schinkel@nki.nl.

ORCID

Alejandra Martínez-Chávez: 0000-0002-6234-172X
Stéphanie van Hoppe: 0000-0001-9094-5814
Alfred H. Schinkel: 0000-0002-4215-8602

Notes

The authors declare the following competing financial interest(s): The research group of Alfred H. Schinkel receives revenue from commercial distribution of some of the mouse strains used in this study. The other authors declare no conflicts of interest.

ACKNOWLEDGMENTS

The authors thank Margarida Martins for assistance in executing the *in vivo* mouse experiments and Ioannis Zavrakidis for advice on statistical calculations and analysis. This research was funded in part by the Mexican National Council for Science and Technology (CONACyT, Scholarship No. 440476).

REFERENCES

(1) Kwapisz, D. Cyclin-Dependent Kinase 4/6 Inhibitors in Breast Cancer: Palbociclib, Ribociclib, and Abemaciclib. *Breast Cancer Res. Treat.* **2017**, *166* (1), 41−54.

(2) Romero, D. Expanding Ribociclib Use. *Nat. Rev. Clin. Oncol.* **2018**, *15*, 470−471.

(3) Tripathy, D.; Bardia, A.; Sellers, W. R. Ribociclib (LEE011): Mechanism of Action and Clinical Impact of This Selective Cyclin-Dependent Kinase 4/6 Inhibitor in Various Solid Tumors. *Clin. Cancer Res.* **2017**, *23* (13), 3251−3262.

(4) Curigliano, G.; Criscitiello, C.; Esposito, A.; Intra, M.; Minucci, S. Pharmacokinetic Drug Evaluation of Ribociclib for the Treatment of Metastatic, Hormone-Positive Breast Cancer. *Expert Opin. Drug Metab. Toxicol.* **2017**, *13* (5), 575−581.

(5) Giacomini, K. M.; Huang, S.-M.; Tweedie, D. J.; Benet, L. Z.; Brouwer, K. L. R.; Chu, X.; Dahlin, A.; Evers, R.; Fischer, V.; Hillgren, K. M.; et al. Membrane Transporters in Drug Development. *Nat. Rev. Drug Discovery* **2010**, *9* (3), 215−236.

(6) Schinkel, A. H.; Jonker, J. W. Mammalian Drug Efflux Transporters of the ATP Binding Cassette (ABC) Family: An Overview. *Adv. Drug Delivery Rev.* **2012**, *64*, 138−153.

(7) Mittal, B.; Tulsyan, S.; Mittal, R. The Effect of ABCB1 Polymorphisms on the Outcome of Breast Cancer Treatment. *Pharmacogenomics Pers. Med.* **2016**, *9*, 47.

(8) Natarajan, K.; Xie, Y.; Baer, M. R.; Ross, D. D. Role of Breast Cancer Resistance Protein (BCRP/ABCG2) in Cancer Drug Resistance. *Biochem. Pharmacol.* **2012**, *83* (8), 1084−1103.

(9) Kuo, T. Roles of Multidrug Resistance Genes in Breast Cancer Chemoresistance. In *Breast Cancer Chemosensitivity*; Yu, D., Hung, M.-C., Eds.; Springer Science: New York, 2007; pp 23−28.

(10) Raub, T. J.; Wishart, G. N.; Kulanthaivel, P.; Staton, B. A.; Ajamie, R. T.; Sawada, G. A.; Gelbert, L. M.; Shannon, H. E.; Sanchez-Martinez, C.; De Dios, A. Brain Exposure of Two Selective Dual CDK4 and CDK6 Inhibitors and the Antitumor Activity of CDK4 and CDK6 Inhibition in Combination with Temozolomide in an Intracranial Glioblastoma Xenograft. *Drug Metab. Dispos.* **2015**, *43* (9), 1360−1371.

(11) de Gooijer, M. C.; Zhang, P.; Thota, N.; Mayayo-Peralta, I.; Buil, L. C. M.; Beijnen, J. H.; van Tellingen, O. P-Glycoprotein and Breast Cancer Resistance Protein Restrict the Brain Penetration of the CDK4/6 Inhibitor Palbociclib. *Invest. New Drugs* **2015**, *33*, 1012−1019.

(12) FDA (Center of drug evaluation and research). *Multidiscipline Review of Ribociclib*; 2017.

(13) Sorf, A.; Hofman, J.; Kučera, R.; Staud, F.; Ceckova, M. Ribociclib Shows Potential for Pharmacokinetic Drug-Drug Interactions Being a Substrate of ABCB1 and Potent Inhibitor of ABCB1, ABCG2 and CYP450 Isoforms in Vitro. *Biochem. Pharmacol.* **2018**, *154*, 10−17.

(14) Elens, L.; Van Gelder, T.; Hesselink, D. A.; Haufroid, V.; Van Schaik, R. H. N. CYP3A4*22: Promising Newly Identified CYP3A4 Variant Allele for Personalizing Pharmacotherapy. *Pharmacogenomics* **2013**, *14* (1), 47−62.

(15) Rochat, B. Role of Cytochrome P450 Activity in the Fate of Anticancer Agents and in Drug Resistance. *Clin. Pharmacokinet.* **2005**, *44* (4), 349−366.

(16) European Medicines Agency. *Assessment Report of Ribociclib*; 2017.

(17) Bakos, E.; Evers, R.; Szakacs, G.; Tusnady, G. E.; Welker, E.; Szabo, K.; de Haas, M.; van Deemter, L.; Borst, P.; Varadi, a.; et al. Functional Multidrug Resistance Protein (MRP1) Lacking the N-Terminal Transmembrane Domain. *J. Biol. Chem.* **1998**, *273* (48), 32167−32175.

(18) Evers, R.; Kool, M.; van Deemter, L.; Janssen, H.; Calafat, J.; Oomen, L. C.; Paulusma, C. C.; Oude Elferink, R. P.; Baas, F.; Schinkel, A. H.; et al. Drug Export Activity of the Human Canalicular Multispecific Organic Anion Transporter in Polarized Kidney MDCK Cells Expressing CMOAT (MRP2) CDNA. *J. Clin. Invest.* **1998**, *101* (7), 1310−1319.

DOI: 10.1021/acs.molpharmaceut.9b00475
Mol. Pharmaceutics 2019, 16, 3842−3852

(19) Poller, B.; Wagenaar, E.; Tang, S. C.; Schinkel, A. H. Double-Transduced MDCKII Cells to Study Human P-Glycoprotein (ABCB1) and Breast Cancer Resistance Protein (ABCG2) Interplay in Drug Transport across the Blood-Brain Barrier. *Mol. Pharmaceutics* **2011**, *8* (2), 571−582.
(20) Jonker, J. W. Role of Breast Cancer Resistance Protein in the Bioavailability and Fetal Penetration of Topotecan. *J. Natl. Cancer Inst.* **2000**, *92* (20), 1651−1656.
(21) Martínez-Chávez, A.; Rosing, H.; Hillebrand, M.; Tibben, M.; Schinkel, A. H.; Beijnen, J. H. Development and Validation of a Bioanalytical Method for the Quantification of the CDK4/6 Inhibitors Abemaciclib, Palbociclib and Ribociclib in Human and Mouse Matrices Using Liquid Chromatography-Tandem Mass Spectrometry. *Anal. Bioanal. Chem.* **2019**, *411*, 5331.
(22) FDA. Guidance for Industry Bioanalytical Method Validation. https://www.fda.gov/files/drugs/published/Bioanalytical-Method-Validation-Guidance-for-Industry.pdf.
(23) European Medicines Agency. Guideline on bioanalytical method validation. https://www.ema.europa.eu/documents/scientific-guideline/guideline-bioanalytical-method-validation_en.pdf.
(24) Schinkel, A. H.; Mayer, U.; Wagenaar, E.; Mol, C. A. A. M.; Van Deemter, L.; Smit, J. J. M.; Van Der Valk, M. A.; Voordouw, A. C.; Spits, H.; Van Tellingen, O.; et al. Normal Viability and Altered Pharmacokinetics in Mice Lacking Mdr1-Type (Drug-Transporting) P-Glycoproteins. *Proc. Natl. Acad. Sci. U. S. A.* **1997**, *94*, 4028−4033.
(25) Jonker, J. W.; Freeman, J.; Bolscher, E.; Musters, S.; Alvi, A. J.; Titley, I.; Schinkel, A. H.; Dale, T. C. Contribution of the ABC Transporters Bcrp1 and Mdr1a/1b to the Side Population Phenotype in Mammary Gland and Bone Marrow of Mice. *Stem Cells* **2005**, *23* (8), 1059−1065.
(26) Van Waterschoot, R. A. B.; Lagas, J. S.; Wagenaar, E.; Van Der Kruijssen, C. M. M.; Van Herwaarden, A. E.; Song, J. Y.; Rooswinkel, R. W.; Van Tellingen, O.; Rosing, H.; Beijnen, J. H.; et al. Absence of Both Cytochrome P450 3A and P-Glycoprotein Dramatically Increases Docetaxel Oral Bioavailability and Risk of Intestinal Toxicity. *Cancer Res.* **2009**, *69* (23), 8996−9002.
(27) van Herwaarden, A. E.; Wagenaar, E.; van der Kruijssen, C. M.M.; van Waterschoot, R. A.B.; Smit, J. W.; Song, J.-Y.; van der Valk, M. A.; van Tellingen, O.; van der Hoorn, J. W.A.; Rosing, H.; Beijnen, J. H.; Schinkel, A. H.; et al. Knockout of Cytochrome P450 3A Yields New Mouse Models for Understanding Xenobiotic Metabolism. *J. Clin. Invest.* **2007**, *117* (11), 3583−3592.
(28) Zhang, Y.; Huo, M.; Zhou, J.; Xie, S. PKSolver: An Add-in Program for Pharmacokinetic and Pharmacodynamic Data Analysis in Microsoft Excel. *Comput. Methods Programs Biomed* **2010**, *99* (3), 306−314.
(29) Gartzke, D.; Delzer, J.; Laplanche, L.; Uchida, Y.; Hoshi, Y.; Tachikawa, M.; Terasaki, T.; Sydor, J.; Fricker, G. Genomic Knockout of Endogenous Canine P-Glycoprotein in Wild-Type, Human P-Glycoprotein and Human BCRP Transfected MDCKII Cell Lines by Zinc Finger Nucleases. *Pharm. Res.* **2015**, *32* (6), 2060−2071.
(30) Samant, T. S.; Dhuria, S.; Lu, Y.; Laisney, M.; Yang, S.; Grandeury, A.; Mueller-zsigmondy, M.; Umehara, K.; Huth, F.; Miller, M.; et al. Ribociclib Bioavailability Is Not Affected by Gastric PH Changes or Food Intake : In Silico and Clinical Evaluations. *Clin. Pharmacol. Ther.* **2018**, *104* (2), 374−383.
(31) Doi, T.; Hewes, B.; Kakizume, T.; Tajima, T.; Ishikawa, N.; Yamada, Y. Phase I Study of Single-Agent Ribociclib in Japanese Patients with Advanced Solid Tumors. *Cancer Sci.* **2018**, *109*, 193−198.
(32) Ward, K. W.; Azzarano, L. M. Preclinical Pharmacokinetic Properties of the P-Glycoprotein Inhibitor GF120918A in the Mouse, Rat, Dog, and Monkey. *J. Pharmacol. Exp. Ther.* **2004**, *310* (2), 703−709.
(33) Duso, B. A.; Trapani, D.; Viale, G.; Criscitiello, C.; D'Amico, P.; Belli, C.; Mazzarella, L.; Locatelli, M.; Minchella, I.; Curigliano, G. Clinical Efficacy of Ribociclib as a First-Line Therapy for HR-Positive, Advanced Breast Cancer. *Expert Opin. Pharmacother.* **2018**, *19* (3), 299−305.
(34) Kwapisz, D. Cyclin-Dependent Kinase 4/6 Inhibitors in Hormone Receptor-Positive Early Breast Cancer: Preliminary Results and Ongoing Studies. *Breast Cancer* **2018**, *25* (5), 506−516.
(35) Patel, Y.; Davis, A.; Kala, A.; Roberts, J.; Jacus, M.; Baker, S.; Roussel, M.; Stewart, C. PDTB-12. CNS Penetration of the CDK4/6 Inhibitor Ribociclib (LEE011) in Non-Tumor Bearing Mice and Mice Bearing Orthotopic Pediatric Brain Tumors. *Neuro. Oncol.* **2016**, *18* (6), 2−3.
(36) Lockman, P. R.; Mittapalli, R. K.; Taskar, K. S.; Rudraraju, V.; Gril, B.; Bohn, K. A.; Adkins, C. E.; Roberts, A.; Thorsheim, H. R.; Gaasch, J. A.; et al. Heterogeneous Blood-Tumor Barrier Permeability Determines Drug Efficacy in Experimental Brain Metastases of Breast Cancer. *Clin. Cancer Res.* **2010**, *16* (23), 5664−5678.
(37) Adkins, C. E.; Mohammad, A. S.; Terrell-Hall, T. B.; Dolan, E. L.; Shah, N.; Sechrest, E.; Griffith, J.; Lockman, P. R. Characterization of Passive Permeability at the Blood−tumor Barrier in Five Preclinical Models of Brain Metastases of Breast Cancer. *Clin. Exp. Metastasis* **2016**, *33* (4), 373−383.
(38) Geoerger, B.; Bourdeaut, F.; DuBois, S. G.; Fischer, M.; Cash, T.; Dobson, J. R.; Marabelle, A.; Robinson, G. W.; Geller, J. I.; Bourdeaut, F.; et al. A Phase I Study of the CDK4/6 Inhibitor Ribociclib (LEE011) in Pediatric Patients with Malignant Rhabdoid Tumors, Neuroblastoma, and Other Solid Tumors. *Clin. Cancer Res.* **2017**, *23* (10), 2433−2441.
(39) Novartis. Pediatric Oncology Subcommittee of the Oncologic Drugs Advisory Committee Briefing Document LEE011. https://www.pharmamedtechbi.com/~/media/Supporting%20Documents/The%20Pink%20Sheet%20DAILY/2013/November/114%20novartis%20preview.pdf.
(40) Patchell, R. A. The Management of Brain Metastases. *Cancer Treat. Rev.* **2003**, *29*, 533−540.
(41) Steeg, P. S.; Camphausen, K. A.; Smith, Q. R. Brain Metastases as Preventive and Therapeutic Targets. *Nat. Rev. Cancer* **2011**, *11* (5), 352−363.
(42) Szakács, G.; Váradi, A.; Özvegy-Laczka, C.; Sarkadi, B. The Role of ABC Transporters in Drug Absorption, Distribution, Metabolism, Excretion and Toxicity (ADME-Tox). *Drug Discovery Today* **2008**, *13* (9−10), 379−393.

DOI: 10.1021/acs.molpharmaceut.9b00475
Mol. Pharmaceutics 2019, 16, 3842−3852